JOURNAL OF OPTOELECTRONICS AND ADVANCED MATERIALS, Vol. 11, No. 11, November 2009, p. 1627 - 1631

Effects of annealing on the structural properties of GaAs-based quantum well solar cells

T. ASAR[a], B. SARIKAVAK[a*], M. KEMAL ÖZTÜRK[a], T. MAMMADOV[a,b], S. ÖZÇELIK[a]
[a]*Department of Physics, Gazi University, 06500 Teknikokullar Ankara, Turkey*
[b]*Azerbaijan National Science Akademy, Physics Institue. Baku Azerbaijan*

$Ga_{1-x}In_xP$ and $In_xGa_{1-x}As$ quantum well solar cells (QWSC) grown on (100) and (110) orientated GaAs substrates were prepared by Molecular Beam Epitaxy (MBE). The annealing effects on the structural properties of the QWSC were investigated by high resolution X-ray diffractometer (HRXRD). Primarily, in-plane and out of-plane lattice parameters were found with the analysis of XRD data. Parallel X-ray strain (ε_{II}), perpendicular X-ray strain ($\varepsilon_{\perp}$), misfit (ε_f), alloy composition (x), tilt values and dislocations of the samples were carried out. Using the determined strain parameters, a dynamical theory based calculations for these structural properties have done by using increasing temperatures bringing out relaxation mechanism; interdiffusion and favored migration.

(Received September 6, 2009; accepted November 12, 2009)

Keywords: Molecular beam epitaxy (MBE), Annealing, Defect anaysis, GaInP, InGaAs

1. Introduction

QWSC is a specific multiple-band gap device between all kinds of heterojunction cells. In the past decades, the developments of quantum well solar cells have generated a great interest. The fundamental principle is such that a quantum well, which is introduced in the intrinsic region of solar cell of wide-band gap material, can be expected to improve the spectral response of the cell in the energy region [1-3]. This response can be adjusted or optimized with proper band engineering [4].

The structural quality of the produced quantum wells can be declared by means of X-ray diffraction which gives rise to characteristic satellite peaks. Not only composition but also the grown layer thickness is very effective for determining dislocations in the material [3, 5]. For determining of these dislocations, high-resolution X-ray diffraction is very appropriate technique and the crystalline quality, strain and misfit can be also calculated by this technique.

In this study, the annealing effects on the structural properties of the SCQW were investigated by HRXRD. Primarily, in-plane and out of-plane lattice parameter were found by analyzing XRD data. Then, parallel strain (ε_{II}), perpendicular strain ($\varepsilon_{\perp}$), misfit (ε_f), alloy composition (x), tilt values and dislocations of the samples were calculated with increasing annealing temperatures bringing out relaxation mechanism; interdiffusion and favored migration from 555 to 720 ^oC by 55 ^oC by using increasing temperatures. A model for the formation of edge dislocations in GaInP and InGaAs QWSCs are proposed at higher temperatures. Each edge dislocation is the result of the combination of two 60° misfit dislocations which have glided from the interface into the substrate [6].

2. Experimental

InGaAs and GaInP quantum well solar cell heterostructures were fabricated on 3-inch diameter epi-ready GaAs (100) and (110) substrate in a V80H-MBE system. The HRXRD measurements were performed by D8-Discover diffractometer equipped on the primary side with a four crystaled Ge (220) monochromator for $CuK_{\alpha 1}$ X-ray beam (λ = 1.5406 Å) and a horizontal divergence slit with a width of 1mm. As regards the Si calibration sample, its best resolution was 16 arcsec. Rocking curves of the sample was measured by $\varpi / 2\theta$ scan (where ϖ and 2θ are the angles of the sample and detector relative to the incident X-ray beam).

Rapid Thermal Annealing was performed in a continuous flow of nitrogen gas in the annealing temperature (Ta) range of 555-775 ^oC by 55 ^oC. The samples were sandwiched between semi-insulating GaAs wafers during annealing to reduce the less of As. The annealing time at each temperature was 40 s. The samples were annealed in N_2 ambient using GaAs proximity caps using rapid thermal processor. The samples were sandwiched between semi-insulating GaAs wafers during annealing to reduce the loss of As.

Sample pictures were taken after annealing at 720 ^oC by Leica CTR 6000. During this process 50x magnification was used. This microscope pictures give

information about surface properties of the sample and they include 1.3 μm scale on each picture.

3. Results and discussion

The structural parameters of the InGaAs and InGaP QWSCs grown on GaAs (100) and (110) substrate by solid source MBE were determined by using HRXRD. Profiles of all symmetric and several asymmetric scans were recorded in ω/2θ scans after optimizing z-height alignment, the tilt angles.

From the sizes and positions of the ω/2θ peaks, one can also deduce the information on crystal imperfections like point defects and dislocations and their interactions, as well as the changes of lattice parameters of the unit cell in a film, caused by misfit strain relaxation. The strain of GaInP and InGaAs layers perpendicular to surface, are conserved on a large scale during growth of these layers.

In the first and second column of the Fig. 1, two peaks and/or their interferences in every scan are observed for GaInP and InGaAs structures. The peaks with higher intensity come from the GaAs substrate. Other peaks originate from GaInP and InGaAs structures. All scans are given to observe the minor changes, determining the structure of defect. From the sizes and positions of the ω/2θ peaks, one can also deduce the information on crystal imperfections like point defects and dislocations and their interactions, as well as the changes of lattice parameters of the unit cell in a film, caused by misfit strain relaxation. In the (220) ω/2θ scans of plane for the GaInP structure, the GaInP peaks with the highest intensities after GaAs peak shift typically to the right and left with increasing temperatures. This case results in the increasing or decreasing of lattice parameters or back or forward moving of (220) planes. In the (224) ω/2θ scans, GaInP peaks approaches to GaAs peak with increasing temperatures. In the (115) ω/2θ scans, crystal quality of GaInP cubic structure is improved at high temperatures and their FWHM values decrease when the intensities of peaks increase at increasing temperatures. For InGaAs structure in the second column of Fig. 1, the second highest InGaAs peak in all ω/2θ scans expand with increasing temperatures and when the peak position affecting strongly the strain behavior shifts, the satellite amplitudes increase firstly then they are decreased or disappeared at higher temperatures, suggesting the degradation of the crystalline nature of the sample, deterioration of the highly abrupt interfaces of the InGaAs [3]. In this case, the roughness of the surface and interface increases. With the increasing internal thermal energy of clusters, defects as the grained structures in the crystal structure are formed and the grain dimensions are become small with the increasing FWHM values of reflection peaks. It is an important result that at increasing temperature, firstly the asymmetric planes more that symmetric ones with higher pole or incline angle according to c-direction of sample are deformed and motives the mosaic defects. This is a common HRXRD result of interdiffusion in our sample [5]. The first decreasing of the satellite peaks' intensity is also attributed to the loss of interface sharpness due to interdiffusion [6].

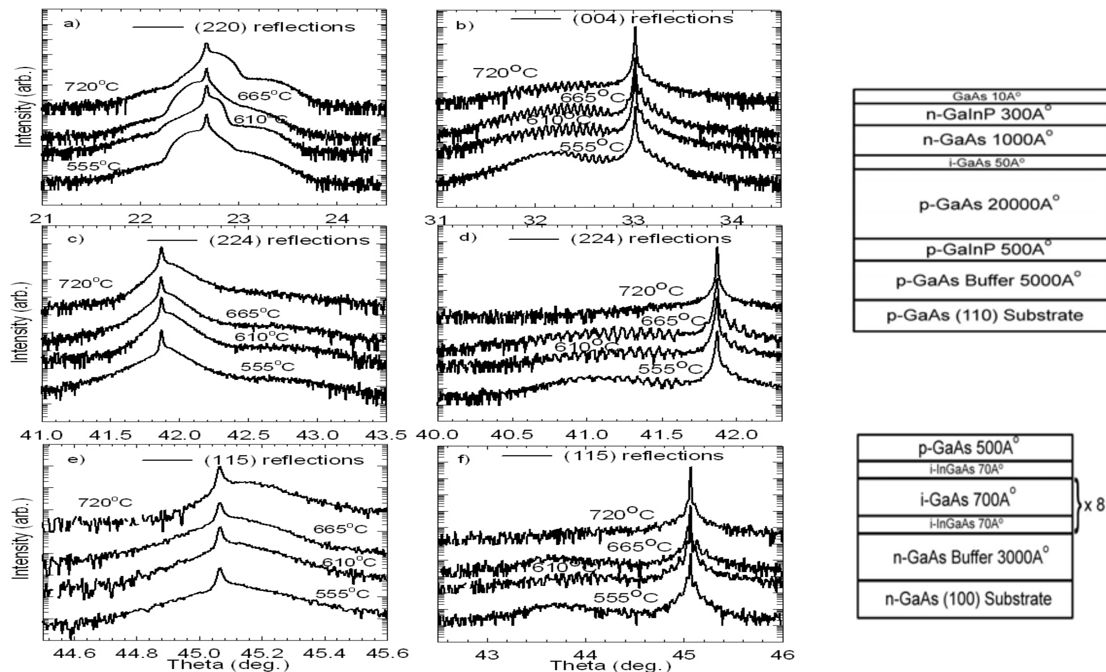

Fig. 1. The ω/2θ scans of the GaInP/GaAs (first column) and InGaAs/GaAs (second column) quantum well solar cells for (a) or (b) (220) or (004), (c) or (d) (115) and (e) or (f) (224) reflections at increasing annealing temperatures. The structures are found in right of the figure.

The lattice parameters $a_{\perp}$ and a_{II} for GaInP and InGaAs structures, which are perpendicular and parallel to the layer plane, respectively, were calculated from the Bragg law with reflection positions by $2\sin\theta_B \cos\varphi = \frac{l\lambda}{a_{\perp}}$ and $2\sin\theta_B \sin\varphi = \frac{\sqrt{h^2+k^2}\lambda}{a_{II}}$ [7,8]. Here, θ_B is Bragg angle, φ is the angle between the diffraction plane and the sample surface, and λ is the wavelength of the X-rays.

The mean lattice parameters for four different azimuth positions were calculated from the reflection positions at the annealed temperatures and then they are used in defect analysis. In different planes of GaInP and InGaAs layer, the graphics for the calculated lattice parameters are drawn in Fig. 2(a) and (b). The lattice parameters in the asymmetric planes show more changing than those of the symmetric planes, which explain the in-plane defects. For InGaAs sample, this degradation becomes quickly at increasing temperatures due to it has quantum well structure defined with satellite peak in the ω/2θ scans. When the lattice parameters of the GaInP structure shows an increasing or decreasing behavior at higher temperatures, in the InGaAs sample, lattice parameters exhibits a waving.

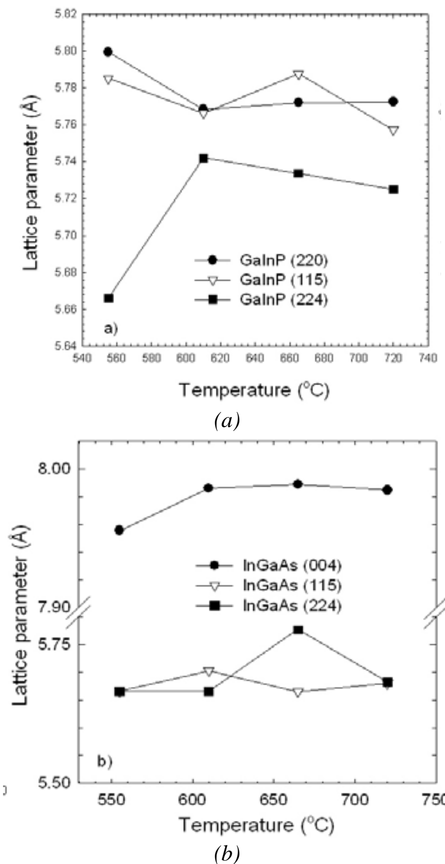

(b)

Fig. 2. The lattice constants calculated from (004), (115) and (224) reflections of the (a) GaInP and (b) InGaAs QWSC samples.

The indium fraction (x) is commonly calculated by Vegard's law. The founded values for x are plotted as depends on the annealing temperatures on Fig. 3(a). When the mosaic defects in InGaP and InGaAs with increasing temperature are increased, the x contends values in the InGaAs show constant behavior but in InGaP shows firstly increase and then becoming decreasing, coming from strain behavior. The interdiffusion due to the composition gradient shows that there is favored migration mechanism to relax the strain energy [9].

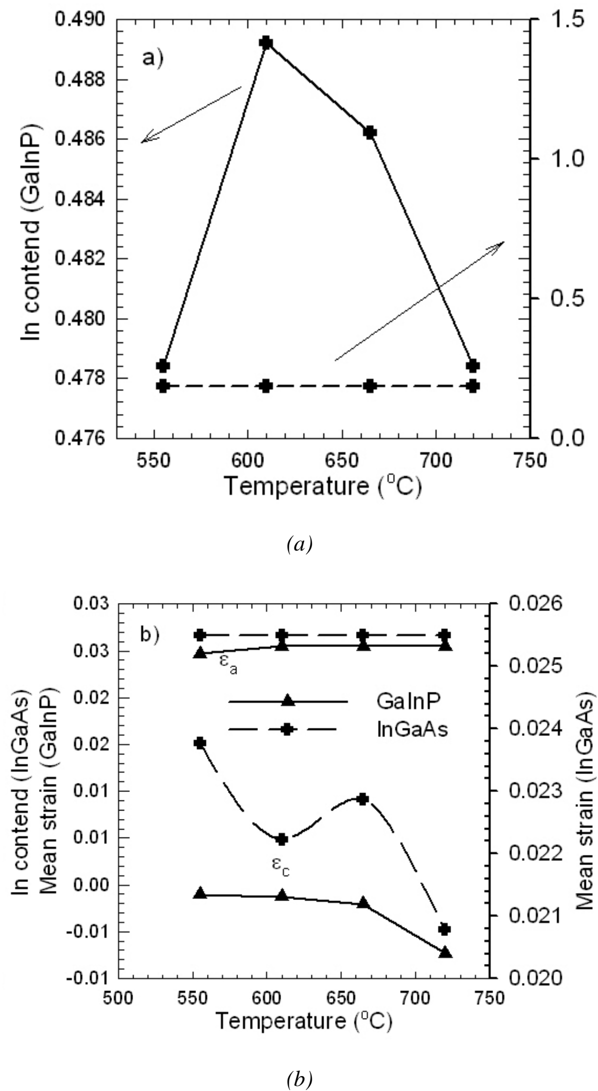

(b)

Fig. 3. The tilt angles versus different annealing temperatures for the ((004), (115) and (224)) and ((220), (115) and (224)) reflections of GaInP and InGaAs structures.

The data obtained using the ω/2θ reflections were analyzed for the out of plane and in-plane strains $\varepsilon_{\perp}$ and ε_{II}, respectively by least square analysis. Perpendicular

(out-of-plane) $\varepsilon_{\perp}$ and parallel (in plane) ε_{II} strains are defined as follows, with respect to the substrate:

$$\varepsilon_c = (\frac{a_c - a_{sub}}{a_{sub}}) \text{ and } \varepsilon_a = (\frac{a_a - a_{sub}}{a_{sub}}) \qquad (1)$$

The ε_c and ε_a strains are defined in Fig. 3(b). The in-plane strains have large values and uniform behaviors more than those of out-plane strains and show the defects of the structure. The out-plane strains show a waving at higher temperatures. At ultimate temperatures, they change more and due to the thickness undulation of GaInP and InGaAs layers and the inhomogeneous indium composition, the strain distribution in the InGaAs layer surface is inhomogeneous, giving rise to a large diffusivity [10]. Effects of these diffusions in every two structure are shown differently in Fig. 6 (a).

From layer to substrate peak separation at these settings, the layer to substrate tilt angle, $T_{L,S}$ is estimated from

$$T_{L,S} = [(\Delta_1 - \Delta_3)^2 + (\Delta_2 - \Delta_4)^2]/4 \qquad (2)$$

where Δ is the peak separation for four azimuthal settings [11-13]. So the tilt between the epitaxial layers and the substrate may change the angular separation between the diffraction peaks. To eliminate the effect of this tilt, three sets of ((004), (115) and (224) scans) and ((220), (115) and (224) scans) were performed at two orientations by rotating the sample by 180° around the [001] axis. The average angular separation of the peaks for each set of scans was calculated.

Tilt angels for every two structure were calculated along planes and were less than 0.1°, and these values are general result [13-15]. Tilt values of asymmetric directions are the lowest one and change more in respect of the symmetric planes. Its reason is that the asymmetric planes are affected very much from strain. Plane tilts of InGaAs structure are affected more than those of GaInP structure with increasing temperatures. Average spacing D of 60° misfit dislocation was calculated from the measured in-plane mismatch using $D = a_s / \sqrt{2}\varepsilon_{II}$ equation.

Average spacing D of 60° misfit dislocation for every two sample were calculated and their values are plotted in Fig. 5(a) and (b). When this value is compared with distance inter two atoms in the lattice, it is very large. Also inverse of it determines the dislocation density ρ=1/D. The calculated dislocation densities for both structures are given in Fig. 5(b). These large values motivates the cross hatch, a morphological defect structure [16]. Fig. 5(b) shows that the dislocation density in GaInP layers is higher than that of InGaAs layer. This case comes from large thermal mismatch between GaInP and GaAs.

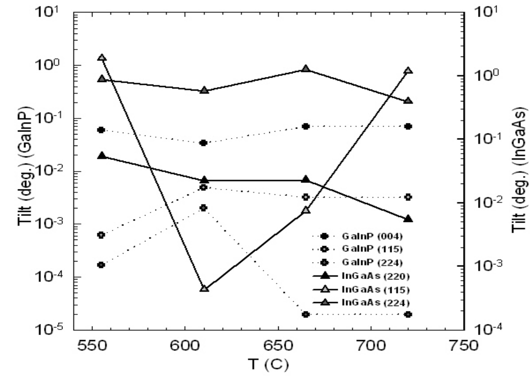

Fig. 4. (a) In contents of InGaP and InGaAs structure; (b) the parallel and perpendicular mean strains of InGaP and InGaAs structures.

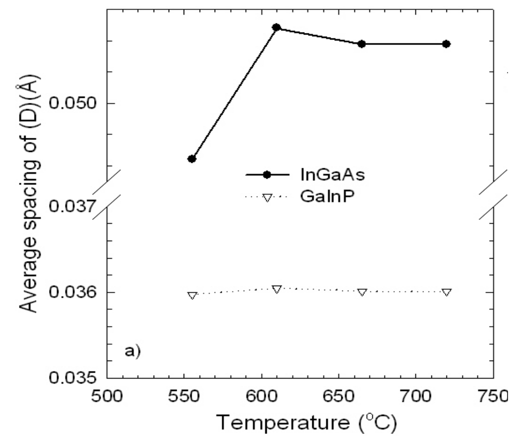

(a)

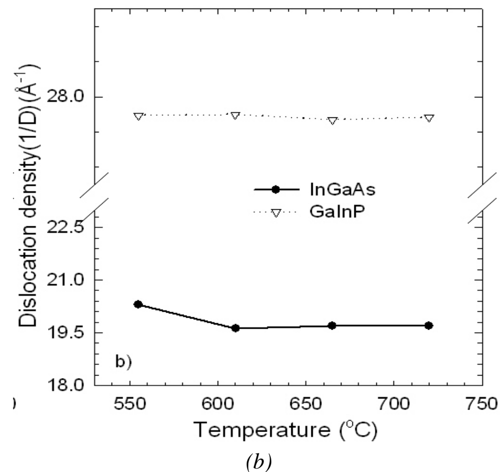

(b)

Fig. 5. (a) Averaging spacing of misfit dislocation and (b) dislocation density in different annealing temperatures for (004), (115) and (224) reflections in GaInP and InGaAs structures.

The thermal annealing was effective in the lattice relaxation and reduction of the defect density. This is expected the enhancement of the dislocation movement by the thermal energy. We have assumed that the defect motion in the lattice- mismatched GaInP and InGaAs layers on GaAs substrates is the same with the dislocation

motion in GaAs layers on Si substrates [16]. After 720 °C annealing temperature, Fig. 6(a) and (b) present the pictures of optic microscope for both GaInP and InGaAs structures. In Fig. 6(a), this annealing temperature brings out high roughness in surface of GaInP structure. In other structure, the defects are occupied as mosaic segmentation.

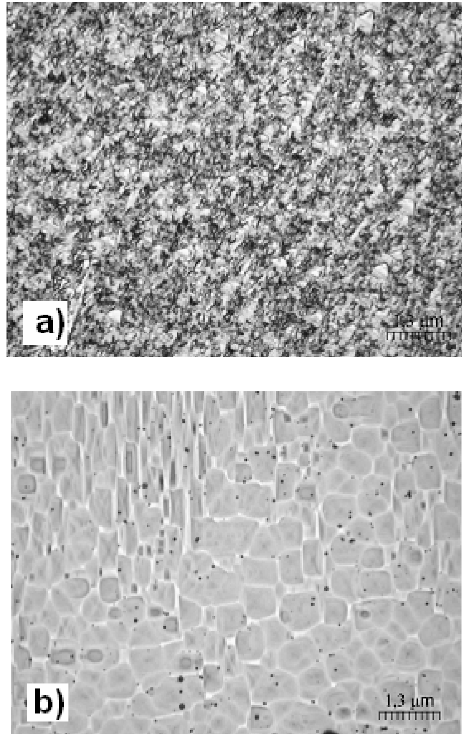

Fig. 6. The microscope surface images at higher annealing temperatures for (a) GaInP and (b) InGaAs heterostructures.

4. Summary and conclusion

After annealing certainly for two samples we found interesting results. In result of annealing we saw different defects in GaInP and InGaAs structure at the same temperatures. Its reason that these structures have different properties such as growth conditions, thickness, indium fraction, etc…). This is important for stability of the sample in high temperatures. Symmetric and asymmetric layers affected in different degrees at these temperatures. Asymmetric peaks are different too. For example in symmetric GaInP and GaInP peaks exists right and left side of GaAs peak. This peak has fluctuations for each ω/2θ scans at every temperature. In ω/2θ scans asymmetric peak slip through GaAs slightly. In InGaAs sample both symmetric and asymmetric InGaAs peaks becoming wider, in asymmetric peaks satellite peaks affected fast and their intensity becoming lower or disappeared.

According to slipping of peak positions on ω/2θ scans we obtained increasing, decreasing or fluctuations on lattice parameters. While In content, which belongs to InGaAs, is changing constantly, In content, which belongs to GaInP firstly increase and then becoming decreasing. Strain in GaInP is lower degree in accordance with InGaAs. Tilt for InGaAs changes big values. Dislocation density for InGaAs has lower value. For surface images GaInP surface has roughness but for InGaAs structure defects appeared like mosaic blocks.

Acknowledgements

This work is supported by DPT under project no 2001K120590.

References

[1] A. Sayari , N. Yahyaoui, A. Meftah, A. Sfaxi, M. Oueslati, J. Lumin. **129**, 105 (2009).
[2] H. C. Liu, F. Capasso, Intersubband Transitions in Quantum Wells, Academic Press, 2000.
[3] S. T. Picraux, B. L. Doyle, J. Y. Tsao, T. P. Pearsall (Ed.), Semiconductors and semimetals, Strained-layer Superlattices: Materials Science and Technology **33**, Academic Press, New York, 1991.
[4] S. B. Lisesivdin, E. Ozbay, Optoelectron. Adv. Mater. –Rapid Comm. **3**(9), 904 (2009).
[5] G. C. Osbourn, J. Appl. Phys. **53**, 1586 (1982).
[6] C. Ulhaqbouillet, A. Lefebvre, Philo. Mag. A **68**, 1273 (1993) .
[7] Y. Takano, M. Masuda, K. Kobayashi, K. Kuwahara, S. Fuke, S. J. Shirakata, J. Crystal Growth **236**, 31 (2002).
[8] S. Dhamodaran, N. Sathish, A. P. Pathak, S. A. Khan, D. K. Avasthi, T. Srinivasan, R. Muralidharan, B. M. Arora, Nucl. Instrum. Meth. B **256**, 260 (2007).
[9] Y. W. Choi, C. R. Wie, K. R. Evans, C. E. Stutz, J. Appl. Phys. **68**, 1303 (1990).
[10] W. J. Bartels, J. Honstra, D. J. W. Lobeek, Acta Cryst. **A42**, 539 (1986).
[11] M. A. Halliwell, M. H. Lyons, S. T. Daves, M. Hockly, C. G. Tuppen, Semicond. Sci. Technol. **4**, 10 (1989).
[12] K. Yuan, K. Radhakrishnan, H. Q. Zheng, Q. D. Zhuang ,G. I. Ing, Thin Solid Films, **391**, 36 (2001).
[13] J. M. Kang, C. S. Son, M. –S. Kim, Y. Kim, S. –K. Min, C. S. Kim, Appl. Phys. Lett. **67**, 641 (1995).
[14] M. A. Moram, M. E. Vickers, M. J. Kappers, C. J. Humphreys, J. Appl. Phys. **103**, 93528 (2008).
[15] J. E. Cunningham, T. H. Chiu, A. Ourmazd, J. Shah, W. T. Tsang, J. Appl. Phys. **60**, 4165 (1986).
[16] M. Yamaguchi, J. Mater. Res. **6**, 376 (1991).

*Corresponding author : beyzas@gazi.edu.tr